© 2018. Published by The Company of Biologists Ltd | Development (2018) 145, dev147793. doi:10.1242/dev.147793

RESEARCH ARTICLE

The primary role of zebrafish *nanog* is in extra-embryonic tissue

James A. Gagnon[1,*], Kamal Obbad[1] and Alexander F. Schier[1,2,3,4,*]

ABSTRACT

The role of the zebrafish transcription factor Nanog has been controversial. It has been suggested that Nanog is primarily required for the proper formation of the extra-embryonic yolk syncytial layer (YSL) and only indirectly regulates gene expression in embryonic cells. In an alternative scenario, Nanog has been proposed to directly regulate transcription in embryonic cells during zygotic genome activation. To clarify the roles of Nanog, we performed a detailed analysis of zebrafish *nanog* mutants. Whereas zygotic *nanog* mutants survive to adulthood, maternal-zygotic (MZ*nanog*) and maternal mutants exhibit developmental arrest at the blastula stage. In the absence of Nanog, YSL formation and epiboly are abnormal, embryonic tissue detaches from the yolk, and the expression of dozens of YSL and embryonic genes is reduced. Epiboly defects can be rescued by generating chimeric embryos of MZ*nanog* embryonic tissue with wild-type vegetal tissue that includes the YSL and yolk cell. Notably, cells lacking Nanog readily respond to Nodal signals and when transplanted into wild-type hosts proliferate and contribute to embryonic tissues and adult organs from all germ layers. These results indicate that zebrafish Nanog is necessary for proper YSL development but is not directly required for embryonic cell differentiation.

KEY WORDS: Nanog, Zebrafish, Maternal-to-zygotic transition, MZT, Yolk syncytial layer, YSL, Zygotic genome activation, ZGA, Lineage tracing, GESTALT

INTRODUCTION

The transcription factor Nanog is part of the core circuitry that regulates mammalian pluripotency (reviewed by Theunissen and Jaenisch, 2014). *In vitro* studies have shown that removal of Nanog triggers differentiation of mouse and human embryonic stem cells (Chambers et al., 2007; Hyslop et al., 2005; Loh et al., 2006; Mitsui et al., 2003). However, a subset of *Nanog* mutant mouse embryonic stem cells are able to self-renew (Chambers et al., 2007). *In vivo* studies have revealed that *Nanog* is required for inner cell mass pluripotency and epiblast development (Mitsui et al., 2003). However, in chimeras with wild-type cells, *Nanog* mutant cells can give rise to tissues from all germ layers (Chambers et al., 2007). Thus, mouse Nanog is involved in, but not absolutely required for, the maintenance of the pluripotent state (Carter et al., 2014; Chambers et al., 2007; Schwarz et al., 2014).

[1]Department of Molecular and Cellular Biology, Harvard University, Cambridge, MA 02138, USA. [2]Center for Brain Science, Harvard University, Cambridge, MA 02138, USA. [3]The Broad Institute of Harvard and MIT, Cambridge, MA 02142, USA. [4]FAS Center for Systems Biology, Harvard University, Cambridge, MA 02138, USA.

*Authors for correspondence (james.gagnon@gmail.com; schier@fas.harvard.edu)

J.A.G., 0000-0003-3978-6058; K.O., 0000-0003-3115-9447; A.F.S., 0000-0001-7645-5325

Received 3 December 2016; Accepted 7 November 2017

The roles of zebrafish Nanog in pluripotency and differentiation are less well-understood. Xu et al. (2012) reported that *nanog* was provided maternally and present in all embryonic and extra-embryonic cells. Morpholino-mediated knockdown of *nanog* mRNA resulted in developmental arrest prior to gastrulation. Nanog morphants displayed defects in the formation of the yolk syncytial layer (YSL), the extra-embryonic tissue that attaches the embryo to the yolk and generates Nodal and BMP signals that pattern mesendoderm (Carvalho and Heisenberg, 2010; Chen and Kimelman, 2000; D'Amico and Cooper, 2001; Hong et al., 2011; Kimmel and Law, 1985; Mizuno et al., 1996; Xu et al., 2012). Gene expression analysis in *nanog* morphants revealed the absence of YSL markers such as *mxtx2* and the misregulation of hundreds of embryonic genes, including Nodal and its target genes. Injecting *mxtx2* mRNA into YSL precursors of *nanog* morphants partially rescued YSL formation and the expression of Nodal and several of its target genes. Although no cell-autonomy data were shown to determine whether Nanog was required in embryonic cells, the study suggested that the primary role of Nanog is to regulate the formation of the YSL (Xu et al., 2012).

Two subsequent studies analyzed potential roles of zebrafish Nanog in embryonic cells (Lee et al., 2013; Perez-Camps et al., 2016). Lee et al. (2013) defined a set of genes expressed at the maternal-to-zygotic transition (MZT), expression of which was reduced in *nanog* morphants. Chromatin immunoprecipitation experiments suggested that many of these genes were direct targets of Nanog (Bogdanovic et al., 2012; Lee et al., 2013; Leichsenring et al., 2013; Xu et al., 2012). Based on the reduced expression of genes in morphants and the Nanog binding data, the study concluded that Nanog, along with Pou5f1 (now known as Pou5f3 in zebrafish) and the SoxB1 family, was involved in the first wave of zygotic transcription in embryonic cells. Subsequent reviews have interpreted these results to conclude that Nanog is directly required for zygotic genome activation in embryonic cells (Langley et al., 2014; Lee et al., 2014; Onichtchouk and Driever, 2016; Paranjpe and Veenstra, 2015), even though the majority of zygotic genes are activated in *nanog* morphants (Lee et al., 2013; Xu et al., 2012). Perez-Camps et al. (2016) reported that morpholino knockdown of *nanog* caused defects in BMP signaling and target gene expression, and suggested that Nanog acts to promote ventral cell-fate specification. Surprisingly, neither study (Lee et al., 2013; Perez-Camps et al., 2016) mentioned the extra-embryonic YSL phenotype of *nanog* morphants (Xu et al., 2012) or tested the postulated direct roles of Nanog in embryonic cells.

Here, we clarify the embryonic and extra-embryonic requirements for Nanog using tissue-specific rescue and chimera analysis. Our results indicate that the primary role of zebrafish *nanog* is YSL formation and that it is not essential for embryonic cell differentiation.

RESULTS

Generation of *nanog* mutants

The interpretation of morpholino experiments can be complicated by potential partial loss-of-function phenotypes and the short half-life of

Development (2018) 145, dev147793. doi:10.1242/dev.147793

morpholinos. To avoid these confounding effects in our studies, we generated *nanog* mutants using transcription activator-like effector nucleases (TALENs) (Carroll, 2014). We isolated an allele containing a 7 bp deletion predicted to cause a frameshift and premature termination codon before the homeodomain required for DNA binding (Fig. 1A). The mutant *nanog* mRNA was not detectable at sphere stage [4 hours post-fertilization (hpf)], presumably owing to nonsense-mediated decay (Fig. 1B). Homozygous zygotic *nanog* (Z*nanog*) mutant embryos showed no phenotypic defects and could be raised to fertile adults. By contrast, maternal-zygotic *nanog* mutants (MZ*nanog*) and maternal-only *nanog* mutants (M*nanog*) arrested at sphere stage, did not undergo normal epiboly (Fig. 1C), and died when embryonic tissue detached from the yolk. The defects observed in MZ*nanog* embryos were rescued by injection of *nanog* mRNA at the 1-cell stage (Fig. 1D). Rescued embryos could be raised to fertile adults, establishing that the observed phenotype is solely due to disruption of the *nanog* gene. The *nanog* mutant phenotype strongly resembles the previously reported *nanog* morphant phenotype (Xu et al., 2012). As M*nanog* and MZ*nanog* mutants had very similar or identical phenotypes, whereas Z*nanog* mutants were viable, we conclude that maternal, but not zygotic, Nanog has essential roles during embryogenesis.

nanog is required for proper formation of the YSL

YSL development and the expression of YSL markers are impaired in *nanog* morphants (Xu et al., 2012). Several lines of evidence indicate that YSL formation is similarly impacted in MZ*nanog* mutants. First, yolk injection of SYTOX Green dye indicated that marginal blastomere nuclei form a normal syncytium in MZ*nanog* at sphere stage (Fig. 2A). However, by 6.5 hpf (shield stage in wild type) these yolk syncytial nuclei are aberrantly clustered together and display an enlarged morphology in MZ*nanog*, reminiscent of the phenotypes caused by microtubule defects in the YSL (Takesono et al., 2012). We next investigated the F-actin band, a network of actin filaments that forms in the YSL during gastrulation and is postulated to promote blastopore closure (Cheng et al., 2004; Köppen et al., 2006; Wilkins et al., 2008). We stained for actin using phalloidin and found that the F-actin band was absent in MZ*nanog* at 8 hpf (Fig. 2B), consistent with the phenotypic arrest in the mutants before epiboly (Fig. 1C). Interestingly, MZ*nanog* embryos still form the shield structure and occasionally exhibit dorsal cell internalization and marginal constriction, even in the absence of epiboly or the F-actin band. These results suggest that YSL formation is initiated in MZ*nanog* mutants but the YSL fails to differentiate properly and maintain the attachment of embryo to yolk.

We next investigated gene expression in the YSL. MZ*nanog* embryos lacked expression of the key YSL determinant *mxtx2* at sphere stage (Fig. 2C). Expression of other YSL marker genes, such as *slc26a1*, *gata3* and *hnf4a* (Xu et al., 2012), was decreased or absent as determined by RT-qPCR (Fig. 2D). RNAseq experiments showed that the expression of many genes expressed in the YSL (Xu et al., 2012) was reduced in MZ*nanog* mutants at 6.5 hpf (Fig. 2E). Expression of many of these genes was not completely eliminated, probably owing to their co-expression in embryonic cells. Compared with zygotically expressed housekeeping genes (Fig. 2F), YSL genes were significantly downregulated in MZ*nanog* embryos (P=7.5×10^{-6}; Fig. 2G). These results confirm and extend previous morphant studies that concluded that Nanog is required for YSL development (Xu et al., 2012).

nanog regulates the expression of a subset of early zygotic genes

nanog morphants were reported to display a widespread reduction in zygotic gene expression (Lee et al., 2013). To determine whether similar defects are found in MZ*nanog* mutants, we used *in situ* hybridization, RT-qPCR and RNAseq. Using *in situ* hybridization and RT-qPCR, we demonstrated that the expression of several early zygotic genes was decreased in MZ*nanog* at sphere stage (Fig. 3A,B). RNAseq experiments confirmed that the expression of many of the previously defined early zygotic genes (Lee et al., 2013) was reduced in MZ*nanog* embryos at sphere stage (Fig. 3C). Compared with maternally provided mRNAs, which are largely unaffected (Fig. 3D), the levels of early zygotic RNAs are significantly reduced in MZ*nanog* mutants (P=0.00307; Fig. 3E). The expression of 79/251 early zygotic genes was reduced >2-fold in MZ*nanog* embryos. Many of these genes are part of

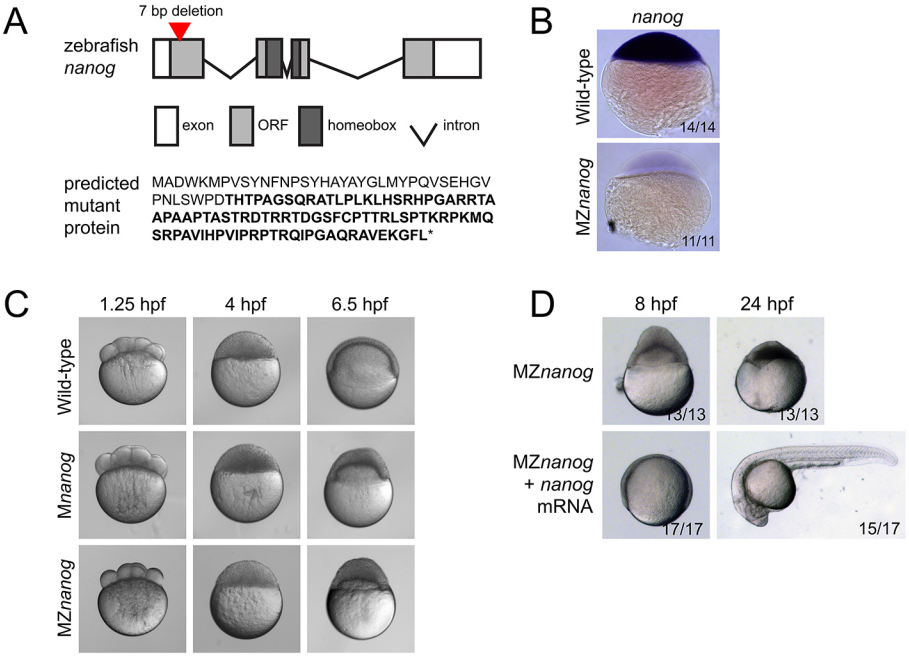

Fig. 1. Generation and phenotype of MZ*nanog* mutants. (A) Top: TALENs were used to generate a 7 bp deletion within the first exon of *nanog*. Exons, introns, the open reading frame (ORF) and the homeobox domain are indicated. Bottom: The predicted mutant protein sequence, with intact amino acids (40 of 384 total) in normal font and frameshifted amino acids in bold font. Asterisk indicates a premature stop codon. (B) *In situ* hybridization for *nanog* expression in wild-type and MZ*nanog* embryos at sphere stage. (C) Wild-type, M*nanog* and MZ*nanog* embryos imaged at 1.25 hpf (8-cell stage), 4 hpf (sphere stage) and 6.5 hpf (shield stage in wild type). Epiboly defects in M*nanog* and MZ*nanog* are apparent at 6.5 hpf. (D) MZ*nanog* embryos are shown at 8 hpf and at 24 hpf, either uninjected or injected with 5 pg *nanog* mRNA at the 1-cell stage. In B and D, the number of embryos exhibiting the illustrated phenotype is shown in the bottom-right corner of each image as a proportion of total embryos examined.

Development (2018) 145, dev147793. doi:10.1242/dev.147793

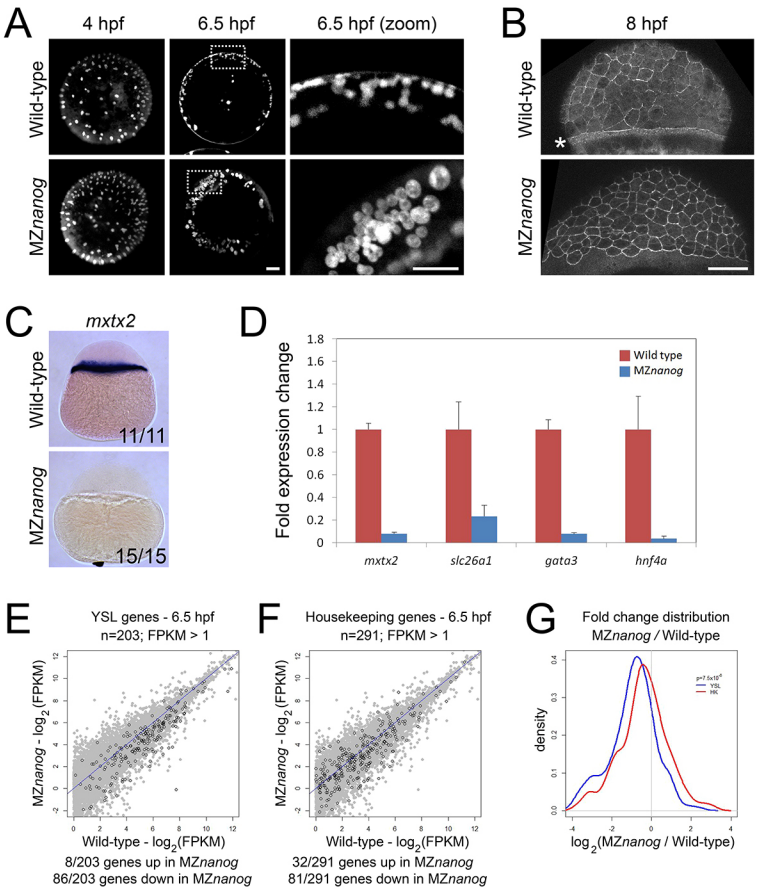

Fig. 2. The YSL is impaired in MZ*nanog* embryos. (A) Yolk syncytial nuclei (YSN) were labeled by SYTOX Green dye injection into the yolk of 128-cell wild-type and MZ*nanog* embryos, and imaged at 4 hpf and 6.5 hpf; *n*=7 for all conditions. Images on the right are magnifications of the boxed areas to the left. (B) The F-actin band, indicated with an asterisk, was visualized using phalloidin staining in fixed wild-type and MZ*nanog* embryos at 8 hpf; *n*=8 for both wild type and MZ*nanog*. (C) *In situ* hybridization for *mxtx2* expression in wild-type and MZ*nanog* embryos at sphere stage. The number of embryos exhibiting the illustrated expression pattern is shown in the bottom-right corner of each image as a proportion of total embryos examined. (D) Fold expression change for *mxtx2*, *slc26a1*, *gata3* and *hnf4a* comparing wild-type and MZ*nanog* embryos at 4 hpf (sphere stage) using RT-qPCR. Error bars show s.d. for three technical replicates (ten embryos per replicate). (E) Differential expression of genes expressed in the YSL, comparing wild type and MZ*nanog* at 6.5 hpf using RNAseq. All genes are in gray, YSL-expressed genes are in black and were previously defined (Xu et al., 2012), and filtered for zygotic expression (Rabani et al., 2014). (F) Differential expression of zygotically expressed housekeeping genes (Lee et al., 2013), comparing wild type and MZ*nanog* at shield stage using RNAseq. All genes are in gray, housekeeping genes are in black. Only those genes with wild-type mRNA expression >1 fragments per kilobase of transcript per million mapped reads (FPKM) are plotted. Genes are categorized as up- or downregulated if their expression in MZ*nanog* differs more than 2-fold from that in wild type. (G) Distribution of fold changes derived from RNAseq data comparing wild-type and MZ*nanog* embryos for all YSL (blue) and housekeeping (HK; red) genes visualized using a kernel density estimation. The displayed *P*-value ($P=7.5\times10^{6}$) comparing these two sets was calculated using a Student's two-tailed *t*-test. Scale bars: 100 µm.

developmental signaling pathways (Table S1). Of the 79 genes reduced in MZ*nanog* mutants, 68 were also significantly decreased in the *nanog* morphants (Lee et al., 2013). These results indicate that *nanog* mutants and morphants have similar gene expression defects.

Expression of *nanog* mRNA in YSL precursors can rescue MZ*nanog* embryos

To clarify the embryonic and extra-embryonic requirements for Nanog, we performed tissue-specific rescue experiments. We first attempted rescue by injection of *nanog* mRNA into the yolk at the 64-cell stage, or directly into the YSL at the 512-cell stage, but observed little to no rescue. We hypothesized that *nanog* expression is required early during embryogenesis, and that delayed expression by mRNA injection at later stages is insufficient to rescue the phenotype. We therefore performed YSL rescue experiments by depositing mRNA in the precursor cells of the YSL by vegetal yolk injection at the 4-cell stage (Xu et al., 2012). Co-injection of GFP mRNA was used to verify that expression was predominantly in the YSL, although we cannot exclude the possibility that low levels of injected mRNA are inherited and translated in embryonic cells (Fig. S1A,B). Similar to 1-cell *nanog* injection, 4-cell yolk injection of *nanog* mRNA was sufficient to rescue the epiboly defects and yolk detachment in most MZ*nanog* mutants (Fig. 4A). Additionally, expression of *mxtx2* and *ndr2* was restored in 4-cell yolk-injected MZ*nanog* embryos (Fig. S1C), indicating that YSL function was rescued. At 24 hpf, the majority of mutants displayed axis rescue, tail elongation, and differentiation of various cell types (Fig. 4B,C). In contrast, injection of *nanog* mRNA into one of 16 cells did not result in any rescue of MZ*nanog* embryos (Fig. 4A,C). We next attempted to rescue MZ*nanog* by *mxtx2* mRNA injection (Xu et al., 2012). Four-cell yolk injection of *mxtx2* mRNA rescued the epiboly defect and yolk detachment in MZ*nanog* mutants (Fig. 4D,E), and some rescued embryos developed differentiated tissues, including somites, notochord, eyes, brain, melanocytes, otoliths and blood. Generally, rescue by *nanog* mRNA was more pronounced than rescue by *mxtx2* mRNA. These results suggest that the primary role of Nanog is in YSL development, and that YSL defects are a major cause of the embryonic phenotypes observed in MZ*nanog* mutants.

nanog mutant cells can undergo epiboly

As an additional test to determine whether *nanog* acts primarily in the YSL, we performed whole blastoderm transplants (Holloway et al., 2009). We transplanted MZ*nanog* blastoderm tissue onto wild-type embryos in which yolk cell was left intact but most of the blastoderm tissue was removed (Fig. 5A). Transplants were performed at the 256- to 512-cell stage, and donor and host tissues were labeled with different fluorescent dyes to track their contributions to the resulting chimera. Shortly after transplantation, we verified that the YSL was exclusively contributed by wild type and that embryonic cells were predominantly contributed by MZ*nanog* tissue (Fig. 5B). Strikingly, these chimeras (*n*=9) underwent epiboly similar to wild-type embryos or wild-type-to-wild-type controls (*n*=10) (Fig. 5C,E). In the reciprocal experiment, we transplanted wild-type blastoderm tissue onto MZ*nanog* embryos in which yolk cell was left intact but most of the blastoderm tissue was removed. These chimeras arrested during epiboly (*n*=5) and had a phenotype similar to MZ*nanog* mutants (Fig. 5D). These experiments cannot rule out an additional role for Nanog in marginal cells but support the idea that Nanog is primarily required in the YSL.

Development (2018) 145, dev147793. doi:10.1242/dev.147793

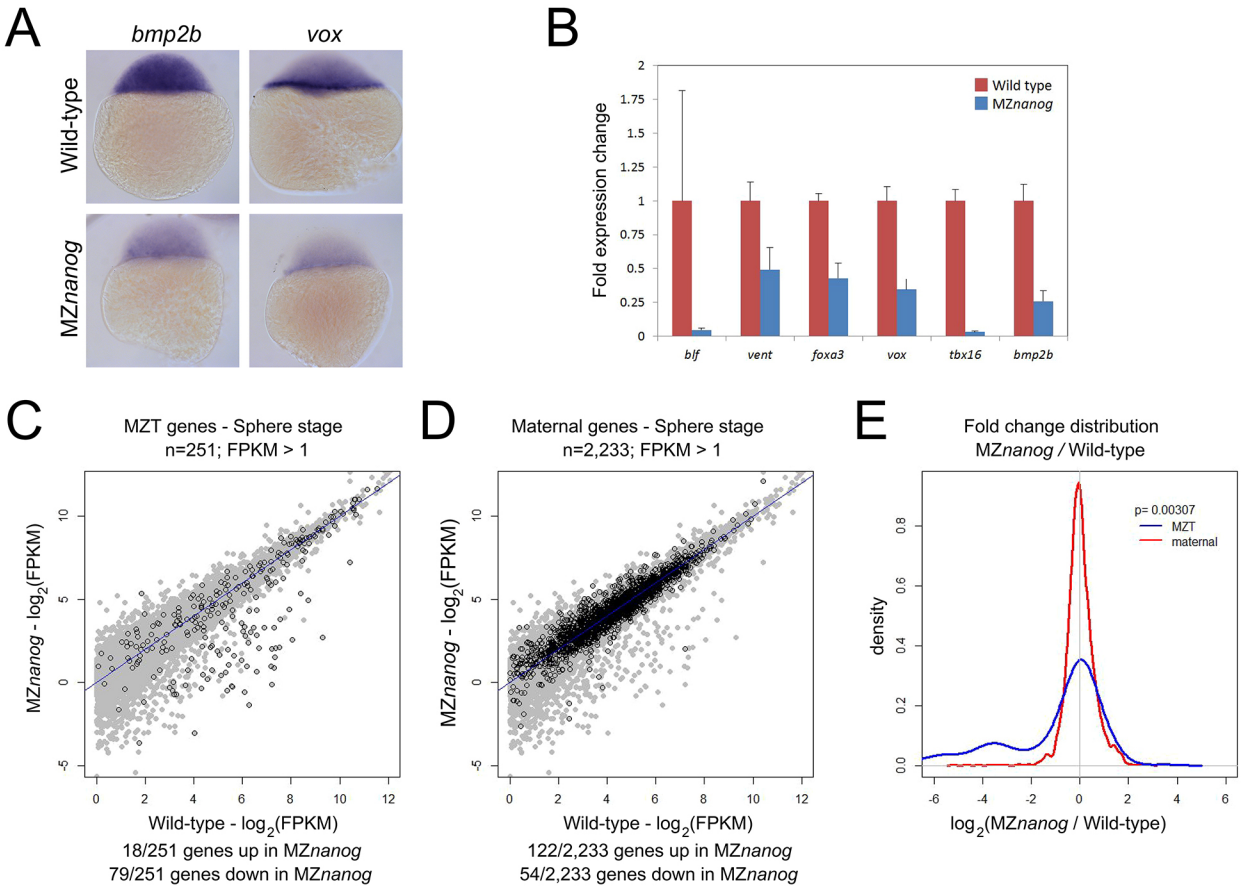

Fig. 3. Defects in early zygotic gene expression in MZ*nanog* embryos. (A) *In situ* hybridization for *bmp2b* and *vox* expression in wild-type and MZ*nanog* embryos at sphere (4 hpf) stage. (B) Fold expression change for the indicated genes comparing wild type and MZ*nanog* at sphere stage using RT-qPCR. Error bars show s.d. for three technical replicates (ten embryos per replicate). (C) Differential expression of early zygotic genes, comparing wild type and MZ*nanog* at sphere stage using RNAseq. All genes are in gray, early zygotic genes (MZT genes) in black were previously defined (Lee et al., 2013). (D) Differential expression of maternally provided genes, comparing wild type and MZ*nanog* at sphere stage using RNAseq. All genes are in gray, maternally provided genes in black were previously defined (Rabani et al., 2014). Only those genes with wild-type mRNA expression >1 FPKM are plotted. Genes are categorized as up- or downregulated if their expression in MZ*nanog* differs more than 2-fold from that in wild type. (E) Distribution of fold changes between wild-type and MZ*nanog* embryos for all early zygotic (blue) and maternal (red) genes visualized using a kernel density estimation. The displayed *P*-value comparing these two sets was calculated using a Student's two-tailed *t*-test.

nanog mutant cells can proliferate and differentiate in wild-type embryos

It has been proposed that Nanog is directly required in embryonic cells (Lee et al., 2013; Perez-Camps et al., 2016), but this assumption has not been tested rigorously. For example, mesendodermal marker gene expression is lost in *nanog* morphants (Lee et al., 2013; Xu et al., 2012) and MZ*nanog* mutants (Fig. 3B, Table S1). Similarly, miR-430 expression and activity are abrogated in *nanog* morphants (Lee et al., 2013). Such defects may be caused directly by absence of Nanog in embryonic cells or indirectly by lack of Nanog in the YSL (Fig. S1C) (Xu et al., 2012). In support of the latter model, MZ*nanog* embryos injected with Nodal (*ndr1*) mRNA can express mesendodermal marker genes at similar levels as in wild-type embryos (Fig. S2). This results reveals that Nanog is not required for Nodal-induced cell-type specification. However, supporting a direct role for Nanog in embryonic cells, we found that a GFP reporter normally silenced by miR-430 is active in MZ*nanog* embryos and in transplanted MZ*nanog* cells (Fig. S3). This result supports a cell-autonomous requirement for Nanog in miR-430 activity.

To test directly the role of Nanog in embryonic cell proliferation and differentiation, we co-transplanted fluorescently labeled MZ*nanog* mutant and wild-type cells into wild-type hosts at sphere stage, and tracked their contributions to the host embryos (Fig. 6A). By 30 hpf, transplanted wild-type and MZ*nanog* mutant cells had proliferated to a similar extent in the host embryo and contributed to many tissues, including brain (ectodermal derivative), muscle (mesodermal derivative) and hatching gland (axial mesodermal derivative) (Fig. 6B). To further test whether cells lacking Nanog can differentiate and contribute to tissues from all three germ layers, we used transgenic markers to follow donor cell differentiation (Fig. 6C), including *fli1a*:GFP (vasculature, a derivative of the mesodermal germ layer), *actc1b*:GFP (trunk muscle, mesodermal germ layer), *isl1*:GFP (trigeminal sensory neurons, ectodermal germ layer) and *sox17*:GFP (gastrointestinal tract, endodermal germ layer) (Higashijima et al., 1997; Lawson and Weinstein, 2002; Sagasti et al., 2005; Sakaguchi et al., 2006) (Fig. S4). We transplanted cells from transgenic M*nanog* embryos into wild-type hosts and found that donor cells proliferated in the host embryo and activated each of the four marker transgenes (Fig. 6D). We additionally found that germ cells were specified in MZ*nanog* embryos, and MZ*nanog* germ cells migrated correctly to the host gonad when transplanted into wild-type host embryos (Fig. S5).

Finally, we tested whether transplanted cells lacking Nanog can make long-term contributions to the adult host. We turned to

Development (2018) 145, dev147793. doi:10.1242/dev.147793

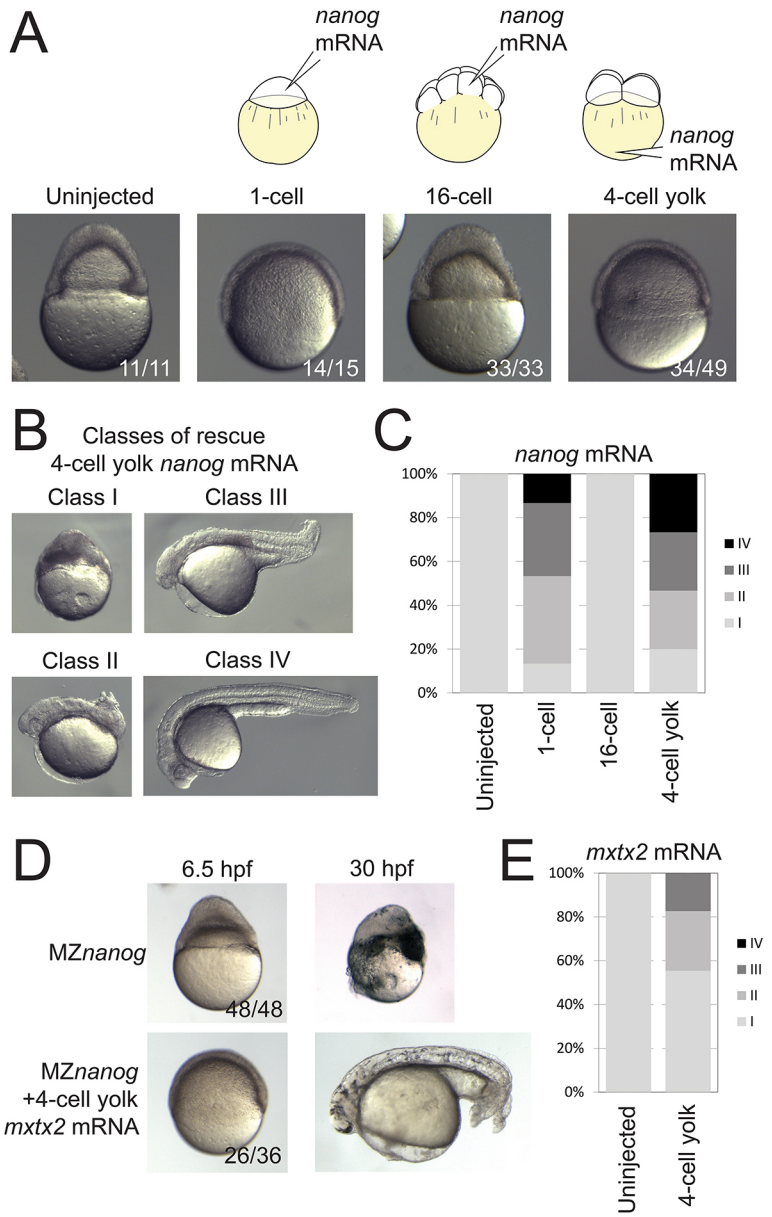

Fig. 4. Rescue of MZ*nanog* embryos by YSL expression of *nanog* or *mxtx2* mRNA. (A) Uninjected MZ*nanog* embryos, or MZ*nanog* embryos injected with 33 pg GFP mRNA and 25 pg *nanog* mRNA into the cell at the 1-cell stage, into a cell at the 16-cell stage, or into the vegetal yolk at the 4-cell stage, were sorted for appropriate spatial GFP expression at sphere stage (as shown in Fig. S1A), and scored and imaged at 8 hpf. (B) Embryos were scored at 24 hpf into four rescue phenotype classes as described in Materials and Methods. (C) Quantification of rescue phenotype scores illustrated as stacked bar plots (uninjected *n*=11; 1-cell *n*=15; 16-cell *n*=33; 4-cell yolk *n*=30). (D,E) Control MZ*nanog* embryos, or embryos injected into the vegetal yolk at the 4-cell stage with 33 pg GFP mRNA and 50 pg *mxtx2* mRNA, were sorted for appropriate spatial GFP expression at sphere stage, scored as above, and imaged at 6.5 hpf and at 30 hpf (D). These scores were quantified and illustrated as stacked bar plots (E) (control *n*=48; 4-cell yolk *n*=92). In A and D, the number of embryos exhibiting the illustrated phenotype is shown in the bottom-right corner of each image as a proportion of total embryos examined.

GESTALT (genome editing of synthetic target arrays for lineage tracing), a long-term lineage-tracing method that uses CRISPR-Cas9 genome editing to introduce permanent mutations in a DNA barcode (McKenna et al., 2016). We injected Cas9 protein and sgRNAs into M*nanog*; GESTALT transgenic embryos to edit the barcode and transplanted cells into wild-type hosts (Fig. 7A). Chimeric embryos were grown to adulthood, and intestine, heart, eyes and brain tissues were isolated. To detect the contributions of M*nanog*; GESTALT cells, GESTALT barcodes were amplified and sequenced from each sample. Across all organs, we found hundreds of barcodes containing different combinations of edits, demonstrating that M*nanog* cells can contribute to adult organs (Fig. 7B). These results reveal that zebrafish Nanog is not required for the proliferation, differentiation or survival of embryonic cells.

DISCUSSION

Our results support the conclusion that the primary role for zebrafish Nanog is in the specification of the YSL (Xu et al., 2012) and that it has no absolutely essential autonomous functions in embryonic cells.

Four lines of evidence support an essential role of Nanog in YSL formation. First, both MZ*nanog* mutants (this study) and *nanog* morphants (Xu et al., 2012) lack expression of *mxtx2*, the master regulator of YSL maturation, as well as expression of several other YSL markers. Second, absence of Nanog blocks formation of the F-actin band within the YSL (Xu et al., 2012) and leads to epiboly defects and embryo detachment (Xu et al., 2012; this study). Interestingly, MZ*nanog* embryos occasionally exhibit marginal constriction, even in the absence of epiboly or the F-actin band. Given the importance of the actin ring for marginal constriction after 50% epiboly (Behrndt et al., 2012; Holloway et al., 2009; Köppen et al., 2006; Popgeorgiev et al., 2011; Wilkins et al., 2008), MZ*nanog* embryos seem to constrict off the yolk by a fundamentally different mechanism. Third, expression of *nanog* mRNA (this study) or *mxtx2* mRNA (Xu et al., 2012; this study) predominantly in YSL precursors partially rescues the YSL gene expression, epiboly and embryonic patterning defects caused by the loss of *nanog*. Fourth, MZ*nanog* mutant yolk and YSL do not support the epiboly movements of wild-type embryonic cells upon

Development (2018) 145, dev147793. doi:10.1242/dev.147793

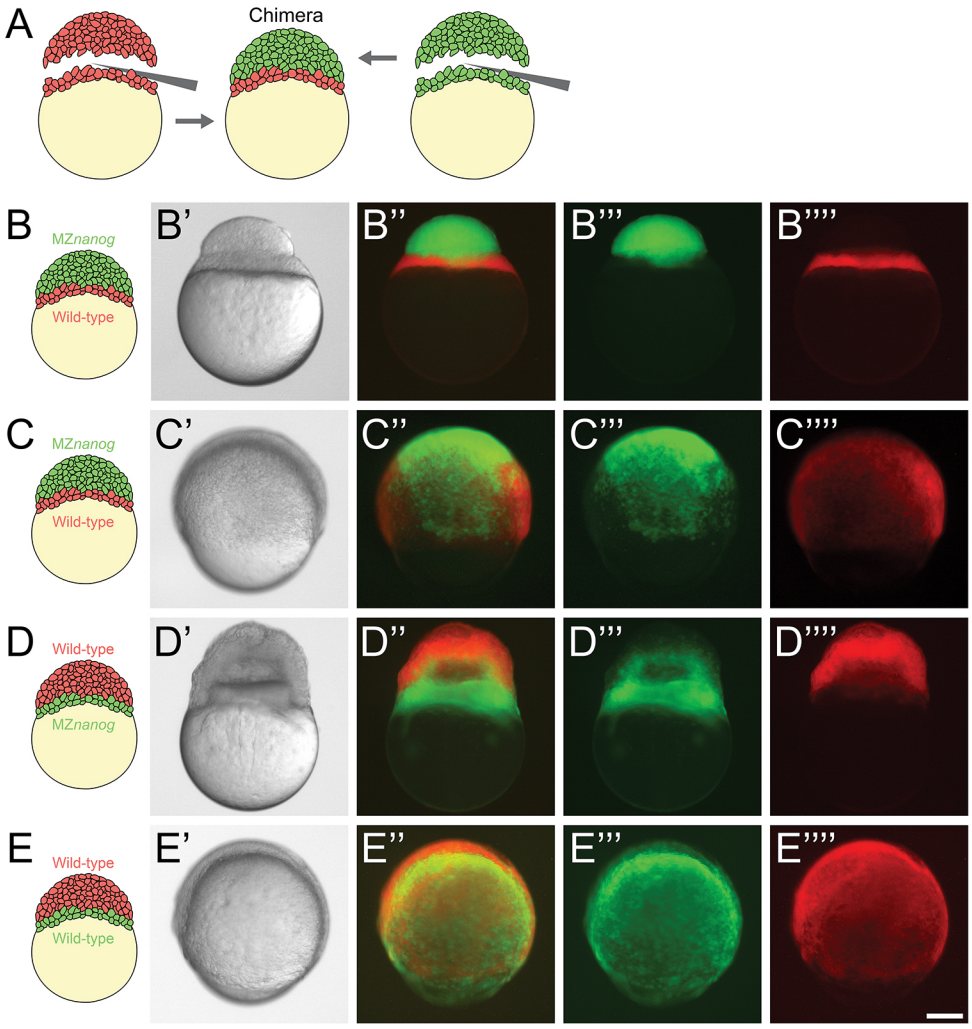

Fig. 5. Blastoderm transplants between wild-type and MZ*nanog* embryos. (A) Diagram of the blastoderm transplant. Donor embryos were injected with dextran-Alexa-488 or dextran-Alexa-546. Blastoderms were separated from yolks and combined to generate chimera embryos. (B) A chimera imaged approximately 15 min after transplant of a wild-type yolk cell and YSL with MZ*nanog* blastoderm (B-B″″), where MZ*nanog* tissue is labeled in green (B‴) and wild-type tissue is labeled in red (B″″). (C) A chimera at 8 hpf of a wild-type yolk cell and YSL with MZ*nanog* blastoderm (C-C″″), where MZ*nanog* tissue is labeled in green (C‴) and wild-type tissue is labeled in red (C″″). (D) A reciprocal chimera at 8 hpf of wild-type blastoderm with MZ*nanog* yolk cell (D-D″″), again with MZ*nanog* tissue labeled in green (D‴) and wild-type tissue labeled in red (D″″). (E) A chimera at 8 hpf of a wild-type yolk cell and YSL with a wild-type blastoderm from a second embryo (E-E″″), where tissue derived from each donor embryo is distinctly labeled (E‴,E″″). Composites of the fluorescent channels are shown in B″, C″, D″ and E″. Scale bar: 100 µm.

blastoderm transplants. These observations strengthen and extend the previously reached conclusion (Xu et al., 2012) that Nanog is essential for proper YSL development.

Four lines of evidence indicate that Nanog is not directly required in embryonic cells. First, *nanog* (this study) or *mxtx2* (Xu et al., 2012; this study) expression predominantly in YSL precursors is sufficient to rescue many aspects of the phenotype, including epiboly, embryo attachment and embryonic cell differentiation. Second, in blastoderm transplants, MZ*nanog* mutant cells undergo epiboly when combined with a wild-type yolk and YSL (this study). Third, MZ*nanog* embryos injected with Nodal (*ndr1*) mRNA can express mesendodermal marker genes to levels similar to wild-type embryos (this study). Fourth, and most unexpectedly, embryonic cells that lack Nanog and are transplanted into wild-type hosts proliferate and differentiate into derivatives of all germ layers and into germ cells (this study). Strikingly, GESTALT-mediated long-term lineage tracing revealed that these cells survive to adulthood in a wild-type host. Together, these observations indicate that Nanog has no absolutely essential autonomous role in embryonic cell differentiation and survival.

Although our results cast doubt on the previously held assumption that Nanog is directly required in embryonic cells for zygotic gene activation (Lee et al., 2013), we did find that MZ*nanog* embryos exhibit embryonic gene expression defects during MZT and that MZ*nanog* mutant cells display reduced miR-430 activity. Seventy-nine genes expressed at sphere stage displayed a 2-fold or greater reduction of transcript levels in MZ*nanog* mutants. Many of these genes encode components of developmental signaling pathways. The gene set reduced in *nanog* mutants broadly overlapped with genes downregulated in *nanog* morphants (Lee et al., 2013). Thus, previously observed gene regulation defects (Lee et al., 2013; Xu et al., 2012) were not simply a consequence of delayed development in morphants. Moreover, maternally provided *nanog* is present throughout the embryo (Fig. 1) (Xu et al., 2012), and Nanog binds promoters of many developmental regulators in the early embryo (Bogdanovic et al., 2012; Lee et al., 2013; Leichsenring et al., 2013; Xu et al., 2012). In agreement with our study, Veil et al. (2018) found that MZ*nanog* cells can contribute to all categorized lineages. By quantification of cell contributions, they concluded that MZ*nanog* cells show reduced potential for contribution to the host. It is not clear whether this reduced potential is due to proliferation or differentiation defects, or an increase in cell death. Although our study shows that Nanog is not strictly required in embryonic cell differentiation, these observations suggest a non-essential contribution of Nanog to the expression of some genes during MZT and in potentiating cell differentiation.

How can the seemingly contradictory observations on the roles of Nanog be reconciled (Lee et al., 2013; Perez-Camps et al., 2016; Xu et al., 2012; Veil et al., 2018; this study)? We suggest the following model. Nanog is primarily required for the proper development of the YSL and the activation of the YSL gene expression program. These genes include patterning signals that in turn regulate gene

Development (2018) 145, dev147793. doi:10.1242/dev.147793

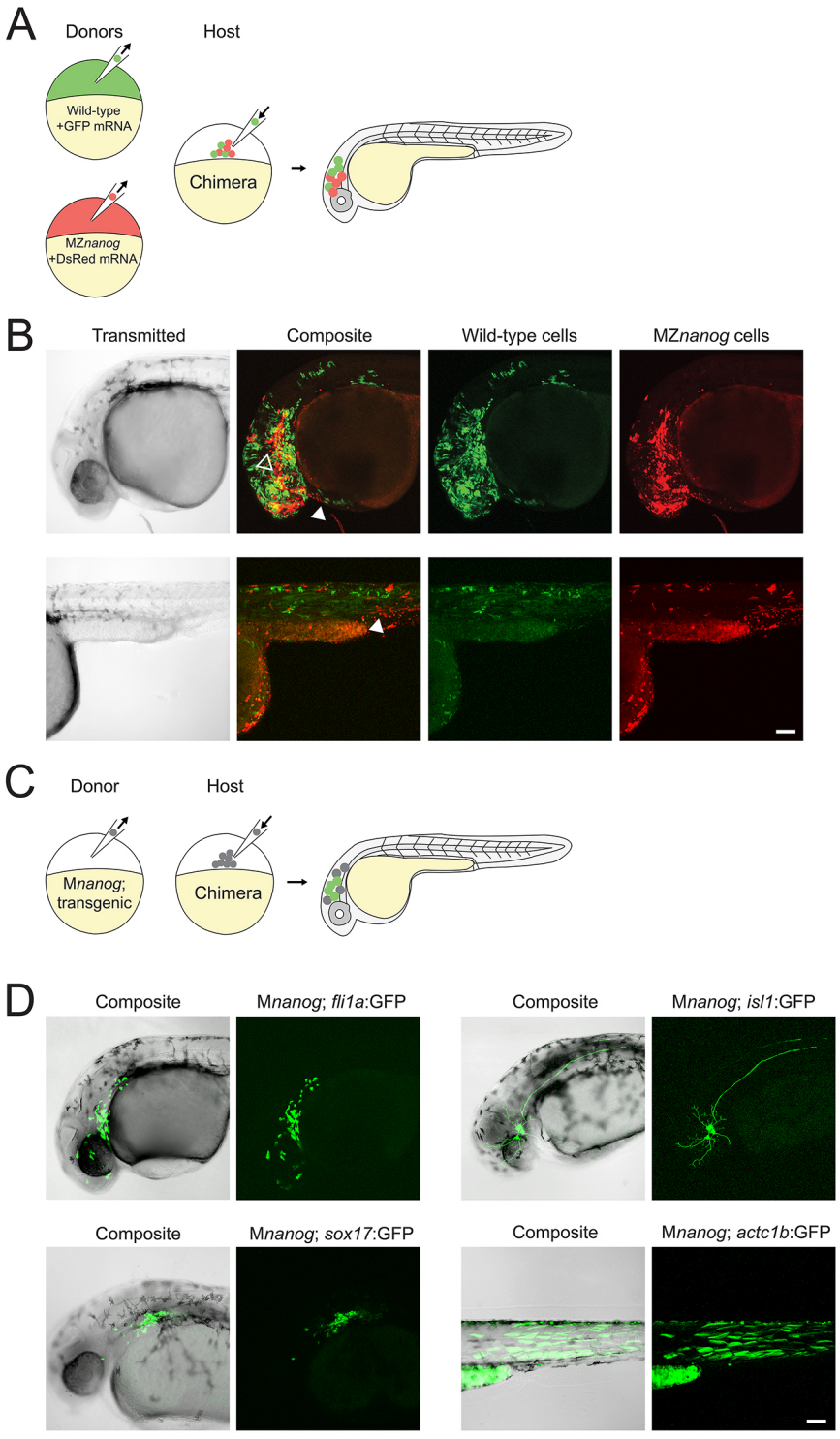

Fig. 6. Transplantation of cells lacking Nanog into wild-type host embryos. (A) Diagram of co-transplantation of wild-type and MZ*nanog* cells into wild-type host embryos, indicating their contribution to the host embryo. (B) Approximately 20 cells were transplanted from donor embryos (at 3-4 hpf) injected at the 1-cell stage with GFP mRNA (wild type) or DsRed mRNA (MZ*nanog*) together into uninjected wild-type host embryos (n=27 across three independent trials). At 30 hpf, embryos were anesthetized, mounted and imaged by confocal microscopy. Two representative embryos are pictured, with arrowheads indicating contributions to eye (black arrowhead, upper row), hatching gland (white arrowhead, upper row), and muscle fibers (white arrowhead, lower row). (C) A diagram of transplantation of M*nanog*; transgenic cells into a wild-type host embryo, with green cells in the host embryo indicating activation of the transgene in transplanted cells. Donor embryos ('M*nanog*; transgenic') were the progeny of a Z*nanog* female crossed to a transgenic male. (D) Approximately 20 cells were transplanted from donor embryos into uninjected wild-type host embryos. At 30 hpf, embryos were anesthetized, mounted and imaged by confocal microscopy. Representative embryos in all panels are displayed as maximum projections from a subset of a *z*-stack, with transgene or tracer expression overlaid onto the other channel or transmitted light channel for context ('Composite'). Transgenic lines used were Tg (*fli1a*:GFP)^{y1} (n=11; Lawson and Weinstein, 2002), Tg (*sox17*:GFP)^{s870} (n=4, Sakaguchi et al., 2006), Tg(*isl1*:Gal4-VP16;UAS:GFP)^{zf154} (abbreviated *isl1*:GFP) (n=16; Sagasti et al., 2005) and Tg(*actc1b*:GFP)^{zf13} (n=5; Higashijima et al., 1997). Wild-type expression patterns for each transgene are shown in Fig. S4 for comparison. Scale bars: 100 µm.

expression in embryonic cells. Nanog is not required for zygotic genome activation and cellular differentiation but binds in conjunction with other pluripotency factors to cis-regulatory regions of embryonic genes, including miR-430, and contributes to their transcription. In this scenario, zebrafish Nanog primarily acts extra-embryonically, and its embryonic requirements might be redundant with other factors and are similar to those in mammals (Carter et al., 2014; Chambers et al., 2007; Schwarz et al., 2014), i.e. involved in but not essential for the acquisition and maintenance of pluripotency and differentiation.

MATERIALS AND METHODS

Animal care

TL/AB strain zebrafish (*Danio rerio*) were used in this study. All vertebrate animal work was performed at the facilities of Harvard University, Faculty of Arts & Sciences (HU/FAS). The HU/FAS animal care and use program maintains full Association for Assessment and Accreditation of Laboratory Animal Care International accreditation, is assured with the Office of Laboratory Animal Welfare (A3593-01), and is currently registered with the United States Department of Agriculture. This study was approved by the Harvard University/Faculty of Arts & Sciences Standing Committee on the Use of Animals in Research & Teaching under Protocol 25–08.

Development (2018) 145, dev147793. doi:10.1242/dev.147793

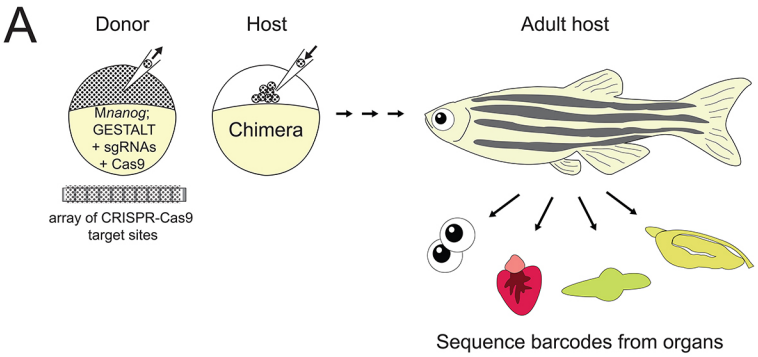

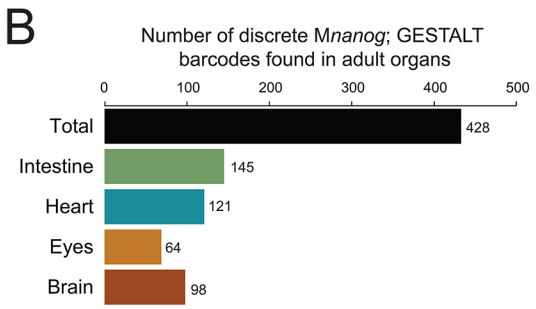

Fig. 7. Long-term GESTALT fate mapping of transplanted cells lacking Nanog. (A) Diagram of cell transplantation at sphere stage from a M*nanog*; GESTALT barcoded donor embryo into a wild-type host embryo. The donor embryo was injected with sgRNAs targeting CRISPR-Cas9 sites in the GESTALT barcode array. Host animals were grown to 90 days post-fertilization, when intestine, heart, eyes and brain were dissected (n=20 animals across two independent trials). Genomic DNA was prepared and barcodes (corresponding to surviving descendants of M*nanog*; GESTALT transplanted cells) were sequenced from each organ. (B) After sequence processing of libraries from each organ across all 20 adults, distinct barcodes corresponding to different clones of transplanted M*nanog*; GESTALT cells were counted. Shown is a summary of all 428 clones of M*nanog*; GESTALT cells found in host animal organs.

Generation of *nanog* mutants

A TALEN pair targeting the first exon of *nanog* (TALEN L: TCCCGAA-TCTGAGCTGGC; TALEN R: TGTGACCCCGCCGGAGTGT) was generated using the TALE Toolbox (Sanjana et al., 2012). Wild-type embryos were injected at the 1-cell stage with 450 pg TALEN pair mRNA. Mutations were verified in injected embryos, and from clutches of outcrossed putative founder adults, by PCR from genomic DNA, followed by T7 Endonuclease I assay (NEB). Mutations within individual founder fish were identified by cloning PCR products followed by Sanger sequencing. An allele containing a 7 bp deletion was isolated and used for all further experiments (a166). These fish were genotyped using a PCR strategy – two allele-specific primers, in combination with a constant primer, separately identify wild-type and mutant alleles. Allele description, and primer and vector sequences can be found in Table S2.

Molecular cloning and *in situ* hybridization

Total RNA was isolated from embryos using EZNA Total RNA kits (Omega Biotek). cDNA was generated using iScript cDNA Synthesis kit (Bio-Rad). Open reading frames for *nanog* and *mxtx2* were amplified by PCR from embryonic cDNA and cloned into the pCS2 vector for generation of mRNA and probes. Open reading frames for *vox* and *bmp2b* were amplified by PCR and cloned using the Strataclone kit (Agilent) for generation of probes. Plasmids encoding GFP, DsRed, *ndr1*, *mxtx2*, *nanog*, GFP-3xPT-miR-430 (Giraldez et al., 2005) and GFP-*nanos1* (Köprunner et al., 2001) mRNAs were transcribed using mMessage mMachine kits (Thermo Fisher). Vector sequences can be found in Table S2. Antisense probes for *in situ* hybridization were transcribed using the DIG RNA labeling kit (Roche). All RNAs were purified using EZNA Total RNA kits (Omega Biotek). *In situ* hybridization was performed as previously described (Thisse and Thisse, 2008); stained embryos were cleared and imaged with a Zeiss Axio Imager.Z1 microscope.

RT-qPCR

Total RNA and cDNA were generated as above. qPCR was conducted using iTaq (Bio-Rad) on a CFX96 (Bio-Rad). Primer sequences are listed in Table S2.

RNAseq

Total RNA was isolated from MZ*nanog* and wild-type embryos at 4 hpf (sphere stage) and 6.5 hpf (shield stage) (n=40 embryos each condition) following a previously published protocol (Pauli et al., 2012). RNA quality was confirmed by Bioanalyzer (Agilent). RNAseq libraries were generated using the TruSeq RNA Library Prep Kit v2 (Illumina) and sequenced on a HiSeq 2500, generating single-end 51 bp reads. Reads were aligned for each sample using TopHat v2.0.13 (Trapnell et al., 2009) with the following command 'tophat -o <output directory> -p 16 –no-novel-juncs -G <gene table> <Bowtie2 genome index> <fastq reads>'. Transcript abundance and differential expression were determined using Cufflinks v2.2.1 (Trapnell et al., 2012) with the following command for each developmental stage 'cuffdiff -p 16 -b <genome.fa -u -L <labels> -o <output directory> <gene table> <wild-type aligned reads .bam file> <mutant aligned reads .bam file>'. Differential gene expression plots were generated in Rstudio. Raw and processed data are available at Gene Expression Omnibus under accession number GSE89245.

YSL staining, expression and phenotypic scoring

YSL nuclei were labeled by injection of 1 nl of 0.5 mM SYTOX Green solution (Thermo Fisher) into the yolk cell at the 128-cell stage, as previously described (D'Amico and Cooper, 2001). F-actin was labeled using Alexa-647-phalloidin (Thermo Fisher), as previously described (Wilkins et al., 2008). Labeled embryos were mounted in 1% low melt agarose and imaged with either a Zeiss Pascal or Zeiss 880 inverted confocal microscope. YSL expression was performed through injection of mRNAs at the 4-cell stage into the vegetal yolk (Xu et al., 2012). Embryos with expression restricted to the YSL were scored and sorted at sphere stage using fluorescence from co-injected GFP mRNA. Phenotypes for all injected embryos were scored during gastrulation and at 24-30 hpf. At 24-30 hpf, classification used the following category definitions (shown in Fig. 4B): Class I, no rescue, ball of necrotic cells or exploded; Class II, axis rescue; Class III, axis rescue and tail extension; Class IV, similar to wild type.

Blastoderm transplantation

Blastoderm transplants were performed as previously described with minor modifications (Holloway et al., 2009). Dechorionated wild-type and MZ*nanog* embryos were injected with 250 pg of either Dextran-Alexa-488 or Dextran-Alexa-546 (Thermo Fisher). Embryos (512-cell stage) were placed in an agarose-coated Petri dish containing 1× Ringer's solution supplemented with 1.6% cleared egg whites, which aids blastoderm adherence. A pulled glass knife was used to remove the blastoderm from the yolk cell of one embryo. This blastoderm was placed

Development (2018) 145, dev147793. doi:10.1242/dev.147793

onto the yolk cell of a recipient embryo using a flamed glass knife. Pressure was applied for a few seconds to adhere the donor blastoderm onto the recipient yolk cell. Embryos were allowed to recover for approximately 10 min before transfer to 1/3× Ringer's solution, and subsequent monitoring and imaging.

Transplantation and imaging

Non-transplanted embryos were anesthetized when necessary, mounted in 3% methylcellulose, and imaged with a Leica MZ 16 F microscope. For transplantation, donor embryos were injected, as appropriate, with either GFP mRNA or DsRed mRNA (50 pg each). Approximately 20-40 cells from a donor embryo were transplanted at sphere stage to a host embryo. Transplant host embryos were screened for fluorescence at 30 hpf with a Leica MZ 16 F microscope, then mounted in 1% low melt agarose and imaged with a Zeiss Pascal confocal microscope.

GESTALT lineage tracing

M*nanog*; GESTALT donor embryos were generated from crosses of homozygous *nanog*$^{-/-}$ female fish to homozygous Tg(ubb:DsRed-barcodev7,myl7:EGFP) male fish (McKenna et al., 2016). These donor embryos were injected with Cas9 protein (NEB) and sgRNAs targeting the v7 barcode (sequence in Table S2) (Gagnon et al., 2014). Transplantation was conducted as described above. Host embryos were grown to adulthood. Intestine, heart, eyes and brain were dissected from euthanized adults and frozen on dry ice. Adult organ gDNA was prepared using the Qiagen DNeasy kit. Sequencing libraries were prepared from each sample using two rounds of PCR to amplify barcodes and attach sample indexes and sequencing adapters (primer sequences in Table S2). Libraries were pooled and subjected to paired-end sequencing on an Illumina MiSeq, using a 500-cycle kit. After demultiplexing, reads were aligned and parsed to determine edited barcode sequences as described (McKenna et al., 2016). To filter sequencing noise, rare barcodes (present at <0.5% abundance per sample) were removed. The number of distinct edited barcodes (containing different combinations of CRISPR-Cas9 edits) present in each sample was counted. Each edited barcode was considered to be derived from the descendants of distinct clones of transplanted cells.

Acknowledgements

We thank members of the Zon lab for the Tg(*fli1a*:GFP) line and helpful discussions; Hazel Sive for a blastoderm transplantation protocol posted on her website; Adam Carte, Jeff Farrell, Jessica Leslie, Nathan Lord, Megan Norris, Andrea Pauli, Michal Rabani, Katherine Rogers and Maxwell Shafer for technical assistance; Marina Veil and Daria Onichtchouk for discussions and sharing their manuscript before publication; Miler Lee and Antonio Giraldez for helpful discussions; and the Harvard Bauer Core Facility, the Biopolymers Facility at Harvard Medical School and the Harvard Center for Biological Imaging.

Competing interests

The authors declare no competing or financial interests.

Author contributions

Conceptualization: J.A.G., A.F.S.; Methodology: J.A.G.; Formal analysis: J.A.G., K.O.; Investigation: J.A.G., K.O.; Writing - original draft: J.A.G.; Writing - review & editing: J.A.G., A.F.S.; Supervision: A.F.S.; Project administration: A.F.S.; Funding acquisition: A.F.S.

Funding

This work was supported by a fellowship from the American Cancer Society (J.A.G.), the Harvard College Research Program (K.O.) and a grant from the National Institutes of Health (HD085905 to A.F.S). Deposited in PMC for release after 12 months.

Data availability

RNAseq data have been deposited in GEO under accession number GSE89245. GESTALT barcode data have been uploaded to the BioProject database with ID PRJNA416917.

Supplementary information

Supplementary information available online at
http://dev.biologists.org/lookup/doi/10.1242/dev.147793.supplemental

References

Behrndt, M., Salbreux, G., Campinho, P., Hauschild, R., Oswald, F., Roensch, J., Grill, S. W. and Heisenberg, C.-P. (2012). Forces driving epithelial spreading in zebrafish gastrulation. *Science* **338**, 257-260.

Bogdanovic, O., Fernandez-Miñán, A., Tena, J. J., de la Calle-Mustienes, E., Hidalgo, C., van Kruysbergen, I., van Heeringen, S. J., Veenstra, G. J. C. and Gómez-Skarmeta, J. L. (2012). Dynamics of enhancer chromatin signatures mark the transition from pluripotency to cell specification during embryogenesis. *Genome Res.* **22**, 2043-2053.

Carroll, D. (2014). Genome engineering with targetable nucleases. *Annu. Rev. Biochem.* **83**, 409-439.

Carter, A. C., Davis-Dusenbery, B. N., Koszka, K., Ichida, J. K. and Eggan, K. (2014). Nanog-independent reprogramming to iPSCs with canonical factors. *Stem Cell Rep.* **2**, 119-126.

Carvalho, L. and Heisenberg, C.-P. (2010). The yolk syncytial layer in early zebrafish development. *Trends Cell Biol.* **20**, 586-592.

Chambers, I., Silva, J., Colby, D., Nichols, J., Nijmeijer, B., Robertson, M., Vrana, J., Jones, K., Grotewold, L. and Smith, A. (2007). Nanog safeguards pluripotency and mediates germline development. *Nature* **450**, 1230-1234.

Chen, S. and Kimelman, D. (2000). The role of the yolk syncytial layer in germ layer patterning in zebrafish. *Development* **127**, 4681-4689.

Cheng, J. C., Miller, A. L. and Webb, S. E. (2004). Organization and function of microfilaments during late epiboly in zebrafish embryos. *Dev. Dyn.* **231**, 313-323.

D'Amico, L. A. and Cooper, M. S. (2001). Morphogenetic domains in the yolk syncytial layer of axiating zebrafish embryos. *Dev. Dyn.* **222**, 611-624.

Gagnon, J. A., Valen, E., Thyme, S. B., Huang, P., Ahkmetova, L., Pauli, A., Montague, T. G., Zimmerman, S., Richter, C. and Schier, A. F. (2014). Efficient mutagenesis by Cas9 protein-mediated oligonucleotide insertion and large-scale assessment of single-guide RNAs. *PLoS ONE* **9**, e106396.

Giraldez, A. J., Cinalli, R. M., Glasner, M. E., Enright, A. J., Thomson, J. M., Baskerville, S., Hammond, S. M., Bartel, D. P. and Schier, A. F. (2005). MicroRNAs regulate brain morphogenesis in zebrafish. *Science* **308**, 833-838.

Higashijima, S.-I., Okamoto, H., Ueno, N., Hotta, Y. and Eguchi, G. (1997). High-frequency generation of transgenic zebrafish which reliably express GFP in whole muscles or the whole body by using promoters of Zebrafish origin. *Dev. Biol.* **192**, 289-299.

Holloway, B. A., Gomez de la Torre Canny, S., Ye, Y., Slusarski, D. C., Freisinger, C. M., Dosch, R., Chou, M. M., Wagner, D. S. and Mullins, M. C. (2009). A novel role for MAPKAPK2 in morphogenesis during zebrafish development. *PLoS Genet.* **5**, e1000413.

Hong, S.-K., Jang, M. K., Brown, J. L., McBride, A. A. and Feldman, B. (2011). Embryonic mesoderm and endoderm induction requires the actions of non-embryonic Nodal-related ligands and Mxtx2. *Development* **138**, 787-795.

Hyslop, L., Stojkovic, M., Armstrong, L., Walter, T., Stojkovic, P., Przyborski, S., Herbert, M., Murdoch, A., Strachan, T. and Lako, M. (2005). Downregulation of NANOG induces differentiation of human embryonic stem cells to extraembryonic lineages. *Stem Cells* **23**, 1035-1043.

Kimmel, C. B. and Law, R. D. (1985). Cell lineage of zebrafish blastomeres: II. Formation of the yolk syncytial layer. *Dev. Biol.* **108**, 86-93.

Köppen, M., Fernández, B. G., Carvalho, L., Jacinto, A. and Heisenberg, C.-P. (2006). Coordinated cell-shape changes control epithelial movement in zebrafish and Drosophila. *Development* **133**, 2671-2681.

Köprunner, M., Thisse, C., Thisse, B. and Raz, E. (2001). A zebrafish nanos-related gene is essential for the development of primordial germ cells. *Genes Dev.* **15**, 2877-2885.

Langley, A. R., Smith, J. C., Stemple, D. L. and Harvey, S. A. (2014). New insights into the maternal to zygotic transition. *Development* **141**, 3834-3841.

Lawson, N. D. and Weinstein, B. M. (2002). In vivo imaging of embryonic vascular development using transgenic zebrafish. *Dev. Biol.* **248**, 307-318.

Lee, M. T., Bonneau, A. R., Takacs, C. M., Bazzini, A. A., DiVito, K. R., Fleming, E. S. and Giraldez, A. J. (2013). Nanog, Pou5f1 and SoxB1 activate zygotic gene expression during the maternal-to-zygotic transition. *Nature* **503**, 360-364.

Lee, M. T., Bonneau, A. R. and Giraldez, A. J. (2014). Zygotic genome activation during the maternal-to-zygotic transition. *Annu. Rev. Cell Dev. Biol.* **30**, 581-613.

Leichsenring, M., Maes, J., Mössner, R., Driever, W. and Onichtchouk, D. (2013). Pou5f1 transcription factor controls zygotic gene activation in vertebrates. *Science* **341**, 1005-1009.

Loh, Y.-H., Wu, Q., Chew, J.-L., Vega, V. B., Zhang, W., Chen, X., Bourque, G., George, J., Leong, B., Liu, J. et al. (2006). The Oct4 and Nanog transcription network regulates pluripotency in mouse embryonic stem cells. *Nat. Genet.* **38**, 431-440.

McKenna, A., Findlay, G. M., Gagnon, J. A., Horwitz, M. S., Schier, A. F. and Shendure, J. (2016). Whole-organism lineage tracing by combinatorial and cumulative genome editing. *Science* **353**, aaf7907.

Mitsui, K., Tokuzawa, Y., Itoh, H., Segawa, K., Murakami, M., Takahashi, K., Maruyama, M., Maeda, M. and Yamanaka, S. (2003). The homeoprotein Nanog is required for maintenance of pluripotency in mouse epiblast and ES cells. *Cell* **113**, 631-642.

Mizuno, T., Yamaha, E., Wakahara, M., Kuroiwa, A. and Takeda, H. (1996). Mesoderm induction in zebrafish. *Nature* **383**, 131-132.

Onichtchouk, D. and Driever, W. (2016). Zygotic genome activators, developmental timing, and pluripotency. *Curr. Top. Dev. Biol.* **116**, 273-297.
Paranjpe, S. S. and Veenstra, G. J. C. (2015). Establishing pluripotency in early development. *Biochim. Biophys. Acta* **1849**, 626-636.
Pauli, A., Valen, E., Lin, M. F., Garber, M., Vastenhouw, N. L., Levin, J. Z., Fan, L., Sandelin, A., Rinn, J. L., Regev, A. et al. (2012). Systematic identification of long noncoding RNAs expressed during zebrafish embryogenesis. *Genome Res.* **22**, 577-591.
Perez-Camps, M., Tian, J., Chng, S. C., Sem, K. P., Sudhaharan, T., Teh, C., Wachsmuth, M., Korzh, V., Ahmed, S. and Reversade, B. (2016). Quantitative imaging reveals real-time Pou5f3-Nanog complexes driving dorsoventral mesendoderm patterning in zebrafish. *Elife* **5**, e11475.
Popgeorgiev, N., Bonneau, B., Ferri, K. F., Prudent, J., Thibaut, J. and Gillet, G. (2011). The apoptotic regulator Nrz controls cytoskeletal dynamics via the regulation of Ca2+ trafficking in the Zebrafish blastula. *Dev. Cell* **20**, 663-676.
Rabani, M., Raychowdhury, R., Jovanovic, M., Rooney, M., Stumpo, D. J., Pauli, A., Hacohen, N., Schier, A. F., Blackshear, P. J., Friedman, N. et al. (2014). High-resolution sequencing and modeling identifies distinct dynamic RNA regulatory strategies. *Cell* **159**, 1698-1710.
Sagasti, A., Guido, M. R., Raible, D. W. and Schier, A. F. (2005). Repulsive interactions shape the morphologies and functional arrangement of zebrafish peripheral sensory arbors. *Curr. Biol.* **15**, 804-814.
Sakaguchi, T., Kikuchi, Y., Kuroiwa, A., Takeda, H. and Stainier, D. Y. R. (2006). The yolk syncytial layer regulates myocardial migration by influencing extracellular matrix assembly in zebrafish. *Development* **133**, 4063-4072.
Sanjana, N. E., Cong, L., Zhou, Y., Cunniff, M. M., Feng, G. and Zhang, F. (2012). A transcription activator-like effector toolbox for genome engineering. *Nat. Protoc.* **7**, 171-192.
Schwarz, B. A., Bar-Nur, O., Silva, J. C. R. and Hochedlinger, K. (2014). Nanog is dispensable for the generation of induced pluripotent stem cells. *Curr. Biol.* **24**, 347-350.
Takesono, A., Moger, J., Farooq, S., Faroq, S., Cartwright, E., Dawid, I. B., Wilson, S. W. and Kudoh, T. (2012). Solute carrier family 3 member 2 (Slc3a2) controls yolk syncytial layer (YSL) formation by regulating microtubule networks in the zebrafish embryo. *Proc. Natl. Acad. Sci. USA* **109**, 3371-3376.
Theunissen, T. W. and Jaenisch, R. (2014). Molecular control of induced pluripotency. *Cell Stem Cell* **14**, 720-734.
Thisse, C. and Thisse, B. (2008). High-resolution in situ hybridization to whole-mount zebrafish embryos. *Nat. Protoc.* **3**, 59-69.
Trapnell, C., Pachter, L. and Salzberg, S. L. (2009). TopHat: discovering splice junctions with RNA-Seq. *Bioinformatics* **25**, 1105-1111.
Trapnell, C., Roberts, A., Goff, L., Pertea, G., Kim, D., Kelley, D. R., Pimentel, H., Salzberg, S. L., Rinn, J. L. and Pachter, L. (2012). Differential gene and transcript expression analysis of RNA-seq experiments with TopHat and Cufflinks. *Nat. Protoc.* **7**, 562-578.
Veil, M. Schaechtle, M. A., Gao, M., Kirner, V. Buryanova, L., Grethen, R. and Onichtchouk, D. (2018). Maternal Nanog is required for zebrafish embryo architecture and for cell viability during gastrulation. *Development* **145**, dev155366.
Wilkins, S. J., Yoong, S., Verkade, H., Mizoguchi, T., Plowman, S. J., Hancock, J. F., Kikuchi, Y., Heath, J. K. and Perkins, A. C. (2008). Mtx2 directs zebrafish morphogenetic movements during epiboly by regulating microfilament formation. *Dev. Biol.* **314**, 12-22.
Xu, C., Fan, Z. P., Müller, P., Fogley, R., DiBiase, A., Trompouki, E., Unternaehrer, J., Xiong, F., Torregroza, I., Evans, T. et al. (2012). Nanog-like regulates endoderm formation through the Mxtx2-Nodal pathway. *Dev. Cell* **22**, 625-638.